

Polarization Issues at CLIC

Ralph W. Assmann* and Frank Zimmermann†
CERN, Geneva, Switzerland

We review polarization issues for CLIC at 3 TeV centre-of-mass energy. An electron beam with about 80% polarization can be produced by an SLC-type photoinjector. Compton scattering off a high-power laser beam may provide a source of positrons with 60%-80% polarization. If the spin transport is taken into account in the geometric layout of the facility and in the choice of local beam energy, no significant depolarization is expected to occur on the way to the collision point. We demonstrate this explicitly by spin tracking through the beam delivery system. During the beam-beam collision itself, due to beamstrahlung and the strong fields at 3 TeV, about 7% of effective polarization will be lost. A polarimeter for the spent beam appears indispensable.

1. Introduction

An accelerator beam consists of an ensemble of particles, that is characterized by the number of particles, the average energy, the charge density, and the average orientation of the particles' spins:

- (1) The *beam energy* determines the direct physics reach of the accelerator facility. Linear colliders provide a path to e^+e^- collision energies above the LEP2 energy of 209 GeV, overcoming the synchrotron radiation limit of e^+e^- storage rings.
- (2) The number of particles and the *charge density* determine the rate of particle-particle collisions, the luminosity. Single-pass collisions remove the standard beam-beam limit, as encountered in storage rings. As a consequence the transverse beam sizes at the collision point can be reduced by three orders of magnitude, compared with those achieved in storage rings. The higher charge density compensates for the lower bunch intensities, fewer bunches, and the lower repetition frequencies.
- (3) The *polarization* of the particle beams can be used to explore the spin dependence of particle interactions. Any information about the spin orientations of the interacting particles can significantly improve the accuracy of important precision measurements. This was demonstrated at the SLC that collided polarized electrons with unpolarized positrons. The electro-weak mixing angle was determined at the SLC with unrivaled precision [1].

Linear colliders preserve polarization to a very high degree. If a polarized beam is injected, it can be brought into collision with only a small loss of polarization. This is in sharp contrast to storage rings, where the polarization drops sharply with beam energy. For example, 57% polarization was measured in LEP with a beam energy of 45 GeV [2]. Beyond this energy, polarization was strongly suppressed, with no measurable polarization at LEP above 60 GeV [2]. There is little hope to extend radiative spin polarization in storage rings to beam energies higher than 80-100 GeV. Linear colliders therefore provide the only path towards polarized e^+e^- collisions at energies above LEP2. All present linear-collider designs consider polarized e^- beams and some of them polarized e^+ beams as well. In this report we discuss polarization issues for CLIC at 3 TeV centre-of-mass energy, and compare them with those for lower energy colliders.

Specifically, we address the following issues: (1) polarized e^- source, (2) polarized e^+ source, (3) spin transport from the source to the collision point and, in particular, the depolarization in the final focus, (4) depolarization during the collision, and (5) polarimetry.

*Ralph.Assmann@cern.ch

†Frank.Zimmermann@cern.ch

2. Polarized Electron Source

Two schemes for a polarized electron source have been proposed:

- a DC gun with laser photocathode (SLC type: *p*-type doped strained GaAs semiconductor photocathode), and
- an rf gun with laser photocathode.

The technical feasibility of the first scheme has been demonstrated, *e.g.* at the SLC. The second scheme is still a research topic [3, 4], and requires major technical breakthroughs, in particular the realization of ultrahigh vacuum in an operating rf gun. In the following, we only discuss the first option, which is well established and can meet the CLIC requirements.

The polarized electron sources used at the SLC [3] as well as those studied at Nagoya University [5, 6] are based on a *p*-type doped strained GaAs photocathode housed in a DC high-voltage gun. The strain splits the energy levels between light and heavy holes allowing for selective excitation and for a polarization in excess of 50%. Treating the surface of the photocathode with Cs and F lowers its work function, so that the vacuum potential drops below the conduction band, and, thereby, increases both the quantum efficiency and the attainable polarization.

The photocathode is characterized by two parameters: the polarization and the quantum efficiency. Both depend on the wavelength of the incident laser. Reducing the wavelength increases the quantum efficiency (typical values: 0.1–1.0%), but lowers the polarization (the maximum value at the SLC was around 80%).

Key issues for the gun are the voltage and the vacuum. A high voltage counteracts the space-charge limit on the electron emission.

The technical design of the gun is closely related to its reliability. At the SLC a loadlock [7] was used to introduce new cathodes or to insert activated photocathodes into the gun. The gun was equipped with Cs channel dispensers [3].

The performance of the polarized electron source can be limited by a number of effects [3]: The space charge field of the electrons limits the charge density that can be extracted. It can be estimated from Gauss' law and is not a limitation for CLIC. A more severe constraint arises from the current limit due to electrons trapped at the surface [8]. The removal rate of these electrons depends on the doping intensity. Higher doping can support a higher current, but degrades the polarization. Both polarization and current specifications can be met in the so-called 'graded doping' scheme [8], where only a thin (10 nm) surface layer of the cathode is doped to a high concentration, *e.g.*, $2 \times 10^{19} \text{ cm}^{-3}$, and the rest of the cathode remains at low doping (10^{18} cm^{-3}). The multibunch operation poses new challenges. The relaxation or recovery time of the photocathode after laser illumination depends on the doping. For $2 \times 10^{19} \text{ cm}^{-3}$ it is about 10 ns [8], or equal to 10% of the CLIC bunch train.

Table I compares various source parameters achieved at the SLC with those required for NLC-II [9] and CLIC. The table demonstrates that the CLIC source is only moderately more demanding than the SLC source, and that it is in every aspect (bunch charge, total charge, pulse current, pulse length) relaxed compared with the NLC-II requirements. Thus, we assume that CLIC can achieve the same polarization level of 80% as has been projected for the NLC.

Table I Comparison of electron source parameters achieved at the SLC with those required for NLC-II [9] and CLIC.

parameter	SLC	NLC-II	CLIC
bunch ch. (10^{10} e^-)	7	2.8	0.4
total ch. (10^{10} e^-)	14	252	62
av. pulse current (A)	0.4	3.2	1.0
pulse length (ns)	62	126	103
beam polarization	~ 80%	~ 80%	~ 80%

Even in the event that the required current cannot be generated from the NLC-type photocathode, a number of back-up solutions exist, such as (1) As capping, which preserves the atomic cleanliness of the cathode surface, (2) increasing the cathode surface, (3) the use of multiple guns, or possibly (4) an alternative photocathode based on two-photon excitation [5].

3. Polarized Positron Source

For the polarized positron source, four schemes have been discussed:

- (1) emission of circularly polarized photons by a high-energy electron beam traversing a helical undulator and subsequent e^+e^- pair creation on a thin target [10, 11, 12],
- (2) the e^+e^- pair creation from backward Compton scattered laser photons [13, 14],
- (3) the collection of high-energetic e^+ from a thin target hit by polarized e^- beam [15],
- (4) laser-Compton scattering in a storage ring, exploiting either spin flip [16, 17], or spin-orbit coupling [18].

The helical undulator scheme was first proposed for VLEPP [10], where a polarization level of 85% was predicted. It was adopted for TESLA with a projected polarization level varying between 40% and 60%. A schematic of the TESLA scheme is shown in Fig. 1.

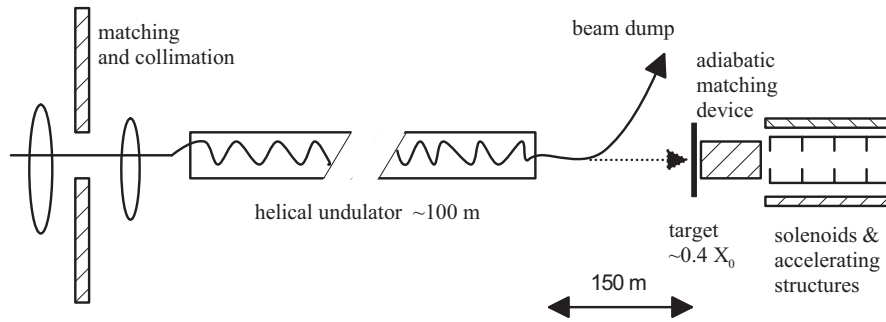


Figure 1: TESLA-style polarized e^+ source consisting of a helical undulator, a thin low-Z target, and a capture section with adiabatic matching. Off-axis photons are scraped prior to the target.

The photon wavelength is $\lambda_\gamma = (3/4)(\lambda_0/\gamma^2)$; the number of quanta is $N_q \approx (\pi/8) (r_e L / (\lambda_0 \lambda_e))$, independent of the beam energy, where λ_0 denotes the period of the undulator. Assuming $\lambda_0 = 1$ cm and an undulator length $L = 300$ m, for a beam energy of $E_b = 100$ GeV the photon energy is $E_\gamma = 6.3$ MeV; for $E_b = 1.5$ TeV, it increases to $E_\gamma = 1.4$ GeV. In either case, the number of quanta emitted per electron is $N_q \approx 170$. If the main electron beam is sent through the undulator prior to the beam-beam collision, energy spread and emittance growth generated in the undulator are a concern.

The use of the undulator scheme at CLIC was studied by T. Kamitani [12]. Considering a total length $L = 150$ m, a field $B_u = 1.76$ T, period $\lambda_u = 3.37$ cm, undulator parameter $K = 5.5$, and $E_1 = 20.0$ MeV, he found that the energy lost by a 1.5-TeV beam is 38.2 GeV, and the additional rms energy spread $\sigma_E/E \approx 1.25 \times 10^{-3}$, which is more than two times smaller than the initial energy spread.

Although the TESLA scheme could thus be used at CLIC, we presently favor the JLC scheme which is based on laser Compton scattering. A historical schematic for JLC is displayed in Fig. 2. Recently, profiting from rapid advances in laser technology, the number of lasers required was reduced by a factor of 10 to about 5 [19]. The laser scheme has several advantages compared with the undulator approach: (1) it decouples the electron and positron beams, (2) it does not require a minimum energy of the electron beam, (3) it does not degrade the beam quality prior to collision, (4) the power requirements are comparable, and (5) experimental tests of this scheme are presently ongoing at the KEK/ATF and experience so far has validated the simulation programs [14].

It may be worth mentioning that in principle the laser parameters can further be relaxed by employing exotic or advanced schemes, *e.g.*, by utilizing plasma channelling to guide and confine the laser light [20]. If the length of the plasma channel is 100 times the Rayleigh length, the laser pulse length could be increased by a factor 100, and the required laser peak power decreased accordingly.

However, the CLIC beam parameters (total charge, current, pulse length) are already more relaxed than those for NLC or JLC, and, thus, the conventional JLC laser-Compton source, presently under experimental demonstration, should suffice. The projected positron polarization level is 60% [20].

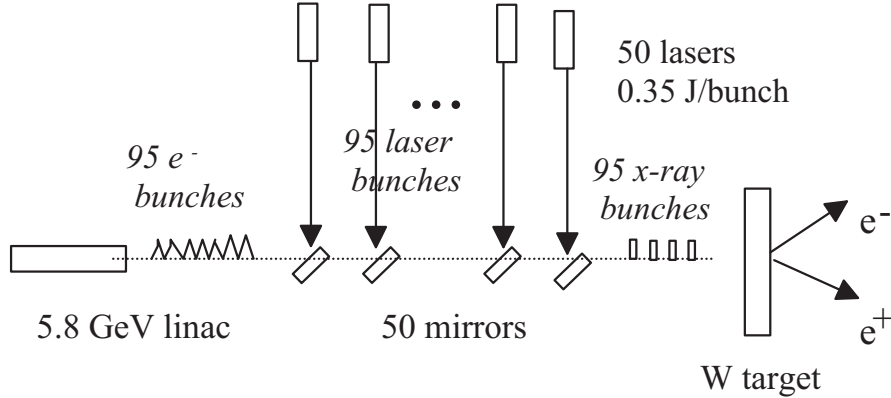


Figure 2: JLC-style polarized e⁺ source, consisting of 50 CO₂ lasers, each producing 95-bunch pulse, scattering off a 6-GeV unpolarized electron beam with 5×10^{10} e⁻/bunch. This results in $N_q \approx 6.6$ γ rays per electron, that are converted into pairs on a W target. Total electric power required is about 15 MW.

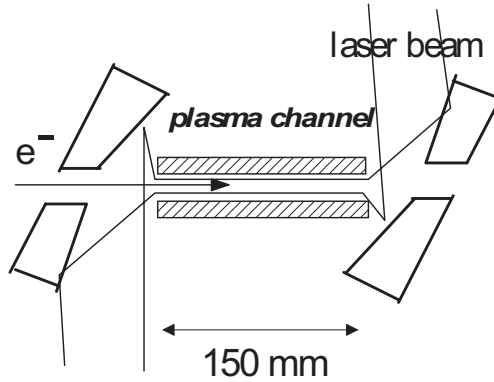


Figure 3: Variant of JLC-style polarized positron source: plasma channeling overcomes the Rayleigh-length limit on the laser pulse duration [20].

Recently another approach was studied at SLAC [15]. A polarized electron beam hitting a thin target produces polarized positrons. The rather low yield ($< 0.1\%$) [15] together with the required number of polarized electrons renders this approach unpromising, however.

Finally, one can directly collide a polarized laser beam and an initially unpolarized positron beam on successive turns in a storage ring. The positron beam will then become polarized either because of (1) direct spin flip [16] or (2) energy loss combined with spin-orbit coupling [18]. Both schemes demand the installation of one or more solenoids with an integrated strength of a few Tesla-meter.

The effect of the direct spin flip appears somewhat controversial (compare Refs. [16] and [18]). Based on the laser-electron cross sections of Ref. [21], the energy γ and the polarization ξ of a positron in the beam after N collisions with circularly polarized photons are given by [16, 17]:

$$\gamma(N) = \frac{\gamma_0}{1 + 2\mu} \quad (1)$$

and

$$\xi(N) = \frac{\mu}{1 + \mu} \quad (2)$$

where $\mu = \gamma_0 \omega_0 N = (4/3)A/(m_0 c^2) \gamma_0 (r_e / \sigma_{ph})^2$ and $\sigma_{ph}^2 = \lambda_0 l_e / (8\pi)$. Here, γ_0 and ω_0 are the initial positron and photon energies, A the laser flash energy, r_e the classical electron radius, and λ_0 and l_e the laser wavelength and full positron bunch length, respectively.

The spin-orbit coupling on the other hand is characterized by the energy dependence of the n axis: $d\vec{n}/d\gamma$. A maximum polarization of about 60% may be reached in this scheme, with a polarization time of [18]

$$\frac{1}{\tau_{pol}} = \frac{10}{7} \frac{d}{dt} \left(\frac{\sigma_E^2}{E^2} \right) = \frac{E_y \Delta E}{E^2 T_{rev}} \quad (3)$$

where E is the beam energy, and ΔE the energy loss per turn. The polarization time can be comparable to the longitudinal damping time, if the laser is used to provide most of the radiation damping.

4. Spin Transport

Once a polarized beam has been produced, it must be transported to the main linac, accelerated, and collided with minimum loss of polarization. Figure 4 shows a schematic of spin manipulations around the damping ring of the NLC, as designed by Emma [9], Minty [22] and Raubenheimer [9]. At injection into the damping ring, the polarization must be in the vertical direction to coincide with the stable spin (\vec{n}) axis of the ring. This is achieved by a combination of dipole magnets with a specific bending angle, which rotates the spin from the longitudinal ('z') into the radial ('x') direction, followed by a solenoid, which further rotates the horizontal spin into the vertical plane ('y'). Likewise, 2 sets of solenoid pairs and one bending section are foreseen downstream of the damping ring, in order to rotate the spin back into the longitudinal direction and to allow for complete control of the average spin orientation at the collision point. Polarization preservation constrains the operating energy of the damping ring. It must be near an odd integer multiple of 220 MeV to avoid depolarizing spin resonances. For completeness, we illustrate the standard accelerator coordinate system in Fig. 5.

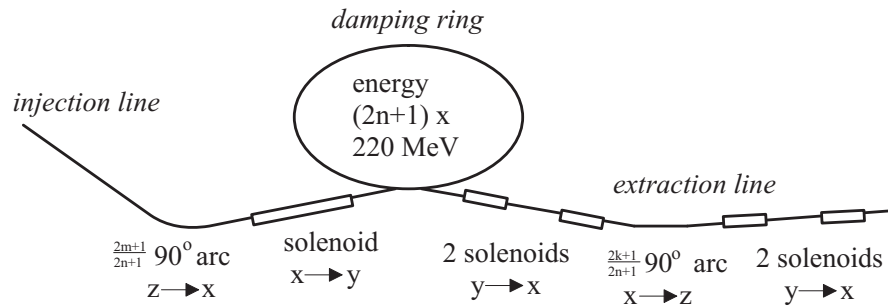


Figure 4: Schematic of spin manipulations around the damping ring à la NLC (P. Emma, M. Minty, T. Raubenheimer et al., 1996).

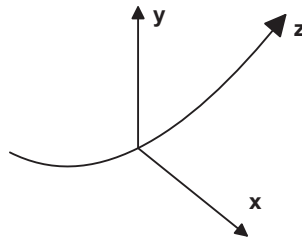


Figure 5: Schematic of the design trajectory in a bending magnet and the coordinate system.

To better understand the spin manipulations and the effect of the bending and solenoid fields, we explicitly give the spin rotations induced by various fields, which follow from the more general

Thomas-BMT equation [23]. A horizontal bending magnet (vertical dipole field) rotates the spin in the $x - z$ plane by an angle

$$\psi_s = a\gamma\theta_B \quad (4)$$

where θ_B is the bending angle and $a = (g - 2)/2 \approx 1.16 \times 10^{-3}$ the anomalous magnetic moment of the electron. For constant bending angle, the spin rotation increases linearly with energy. A longitudinal solenoid field rotates the spin in the $x - y$ plane, by an angle

$$\psi_s = \left[1 - \left(\frac{g - 2}{2} \right) \right] \frac{B_z L_s}{B\rho} \approx \frac{B_z L_s}{B\rho} \approx 2\psi_b, \quad (5)$$

where ψ_b is the transverse roll angle

The polarization decreases also due to the intrinsic beam energy spread σ_δ if there is a net bending angle. This depolarization is expressed by

$$P/P_0 = \exp(-(\psi_s \sigma_\delta)^2 / 2) \quad (6)$$

with σ_δ the rms energy spread. If the angle $\psi_s \neq 0$, then unavoidably also $\Delta P \neq 0$. Two numerical examples may illustrate the magnitude of the depolarization. Considering a beam energy of 9 GeV, near the second bunch compressor of CLIC, a bending angle of π , and an rms energy spread of $\sigma_\delta = 0.2\%$, the depolarization is $\Delta P \approx 1\%$. In the final focus at 1.5 TeV beam energy, considering the nominal rms energy spread $\sigma_\delta = 0.28\%$ and a bending angle θ_B of 10 mrad (half the crossing angle), we find $\Delta P \approx 0.5\%$.

The spin transport in the CLIC beam delivery can be estimated with greater precision using numerical tracking. For a particle distribution ($i = 1, N$) we define a classical spin vector \vec{S}_i for each particle. The particles are tracked through the beam delivery at the nominal beam energy of 1500 GeV, corresponding to $a\gamma = 3404$. Transverse fields that deflect the particle by an angle θ then cause a spin rotation which is $a\gamma = 3404$ times larger. For simplicity we approximate $(a\gamma + 1)$, as it should be used for quadrupoles, with $a\gamma$. This approximation introduces only very small errors, as long as $\theta \ll 1$. Taking into account all transverse fields (bending magnets and quadrupoles) in the beam delivery, the rotation of the individual spin vectors can be calculated using the Thomas-BMT equation [23]. The polarization vector is then obtained as the average of all individual spin vectors:

$$\vec{P} = \begin{pmatrix} P_x \\ P_y \\ P_z \end{pmatrix} = \frac{1}{N} \sum_{i=1}^N \vec{S}_i. \quad (7)$$

The degree P of polarization is defined as the length of the polarization vector:

$$P = |\vec{P}|. \quad (8)$$

For the spin tracking studies, we consider two different design schemes for the CLIC beam delivery system:

- (1) The baseline solution: The baseline optics [24] considered here comprises a semi-conventional final focus [25], and is 3.1 km long. We assume that the collimation system can at least partly be integrated into this system.
- (2) The advanced or compact solution: This scheme comprises a compact final focus with nonzero dispersion across the final doublet [26, 27], whose length is only 400 m. Upstream of the compact final focus we have added a comprehensive 5.5-km long cleaning and protection system, scaled from the 1-TeV NLC design [28], in which both energy and betatron collimation are performed.

We track 10000 particles using the MAD program [29], in order to obtain the phase-space coordinates behind each beam-line element. In a second step, we compute the evolution of the single-particle spin vectors and their average from the individual phase-space trajectories.

The initial particle coordinates chosen are representative of the CLIC beam. In the transverse phase space the particle distributions are taken to be Gaussians with rms beam sizes corresponding to the CLIC design emittances of $\gamma\epsilon_x = 0.68 \mu\text{m}$ and $\gamma\epsilon_y = 0.02 \mu\text{m}$. In the longitudinal phase space, we have assumed a Gaussian spatial profile as well (irrelevant for this study) and a flat energy spread extending from -0.4% to $+0.4\%$, which is a fair approximation to the shape predicted by linac simulations [30].

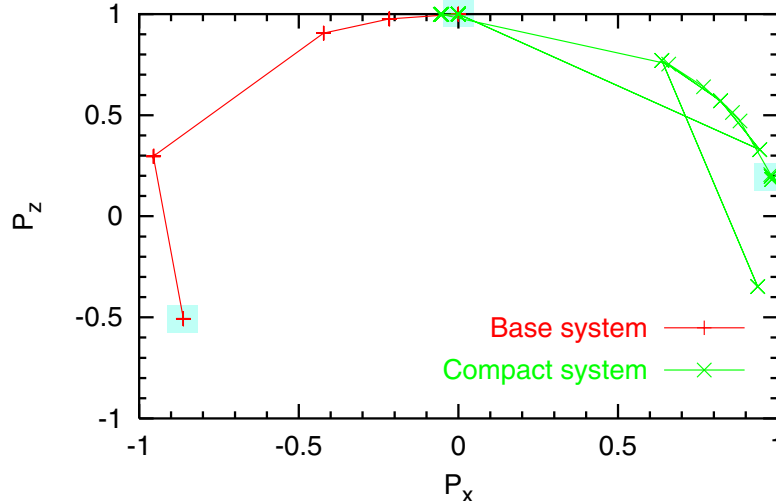


Figure 6: Rotation of the polarization vector in the x-z plane in the short and base CLIC final-focus system. The initial ($P_x = 0, P_z = 1$) and final polarization values are indicated by underlaid boxes.

The rotation of the polarization vector in the x-z plane is shown in Figure 6 for both beamlines. All particles start with longitudinal spin vectors $S_i = (0, 0, 1)$, therefore $P_z = 1$. For physics purposes the polarization vector should point into the longitudinal z-direction. Due to the design vertical dipole fields it is, however, strongly rotated into the horizontal direction, leaving for both CLIC beam delivery designs a very much reduced level of longitudinal polarization ($P_z < 50\%$). It is evident that the polarization vector must be "matched" into the beam delivery system, requiring specific non-zero values for the horizontal and longitudinal polarizations.

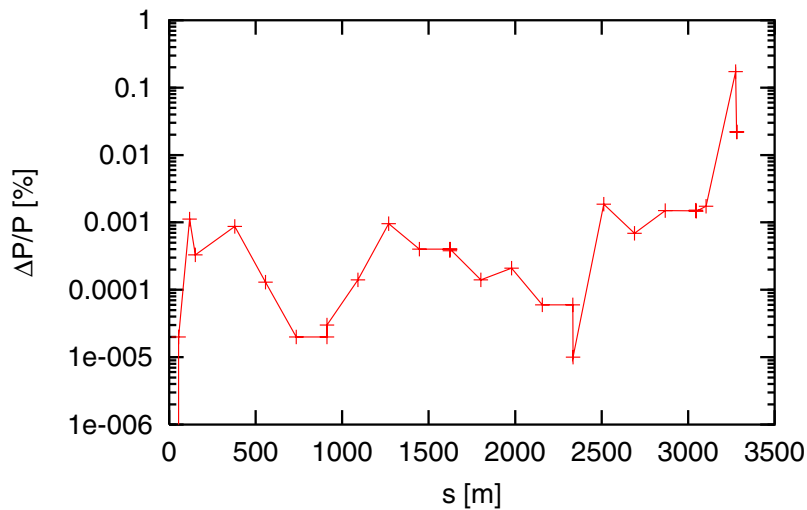


Figure 7: Depolarization versus longitudinal position s due to the transverse magnetic fields in the baseline solution of the CLIC final focus.

The beam can be depolarized if the individual particle spins are rotated differently. This hap-

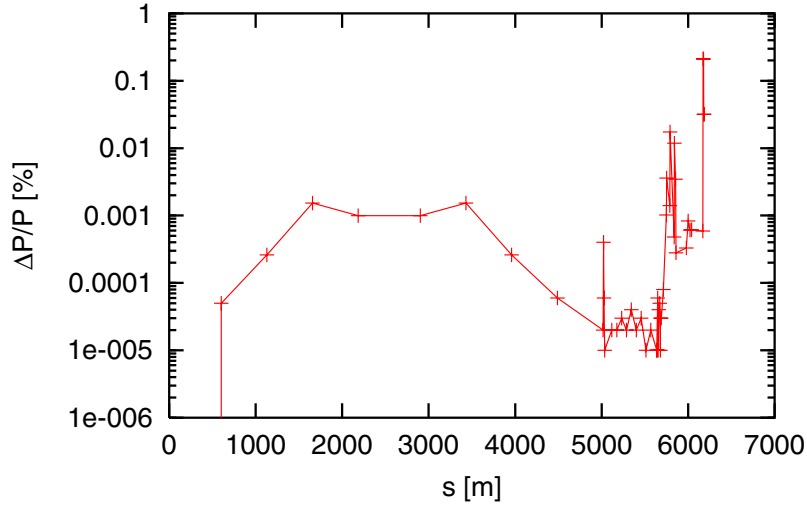


Figure 8: Depolarization versus longitudinal position s due to the transverse magnetic fields in the compact CLIC final focus with collimation section.

pens due to the final beam size in the quadrupoles (particles at small amplitudes are almost unperturbed, while particles at large amplitudes in the tails of the beam can experience strong spin rotations) or due to beam energy spread in the bending magnets. Here, we calculated the depolarization due to those two effects and for both the short and baseline beam delivery solutions. The results are shown in Figures 7 and 8. As expected, the depolarization is strongest at the final doublets, where the spot size and the quadrupole strengths are largest. The final depolarization in the two beamlines is 0.02–0.03%. We conclude that the expected depolarization from transverse fields in the beam delivery systems of CLIC is small and can be neglected for practical purposes.

5. Depolarization during Collision

The effective polarization decreases during the beam-beam collision. In a storage-ring collider the strength of the collisions is measured in terms of the beam-beam tune-shift parameter ξ . For a linear collider, it is characterized by the disruption parameters $D_{x,y}$. The two parameters are related via

$$\xi_{x,y} = \frac{\beta_{x,y}^*}{\sigma_z} D_{x,y} = \frac{2Nr_e\beta_{x,y}^*}{\gamma\sigma_{x,y}(\sigma_x + \sigma_y)}. \quad (9)$$

At the interaction point of a linear collider, particles emit synchrotron radiation in the field of the opposing beam, known as ‘beamstrahlung.’ Its magnitude is measured by the parameter Υ , referring to the critical photon energy $\hbar\omega_c$, and by N_y , denoting the number of photons emitted per beam particle. These two quantities are expressed as

$$\Upsilon = \frac{2}{3} \frac{\hbar\omega_c}{E} \approx \frac{5}{6} \frac{\gamma r_e^2 N_b}{\alpha\sigma_z(\sigma_x + \sigma_z)} \quad (10)$$

and

$$N_y \approx \frac{5}{2} \frac{\alpha\sigma_z}{\gamma\lambda_e} \Upsilon \left[\frac{1}{(1 + \Upsilon^{2/3})^{1/2}} \right] \approx 2 \frac{\alpha r_e N_b}{\sigma_x + \sigma_y} \quad (11)$$

where N_b is the bunch population, α the fine structure constant, and $\sigma_{x,y}$ the rms transverse beam size.

Table II compares the parameter values of ξ , Υ and N_y for CLIC with those achieved at the SLC and envisioned for NLC. Clearly, the collisions are strongest for CLIC, both in terms of field

Table II Comparison of the collision strength for SLC, NLC and CLIC.

parameter	symbol	SLC	NLC	CLIC
b.b.-parameter	$\xi_{x,y}$	1	8	30
Upsilon	Y	2×10^{-3}	0.3	8.1
photons per e^- (e^+)	N_y	1	1.4	2.3

strength and in terms of synchrotron radiation. Therefore, the depolarization at CLIC will be larger than in the other two systems.

Two processes contribute to the beam-beam depolarization:

- The first process is spin-flip radiation. Its magnitude can be estimated by [31]

$$\Delta P = 2N_y U_{f0} \quad (12)$$

where the function $U_{f0} = U_{f0}(Y)$ is depicted in Ref. [31]. For $Y \approx 8$ and $N_y \approx 2.3$, one finds the value $U_{f0} \approx 0.02$ [31], from which we deduce that the total depolarization after the collision is about $\Delta P \approx 10\%$. The more relevant luminosity-weighted effective depolarization [32] is $[\Delta P] \approx 0.27 \cdot \Delta P \approx 2.7\%$.

- The second process is spin precession in the beam magnetic field. The depolarization formula is [31]

$$\Delta P \approx 0.006(N_y/U_0)^2 \quad (13)$$

Inserting $N_y \approx 2.3$ and $U_0 \approx 0.5$ one finds $\Delta P \approx 13\%$ and, for the luminosity-weighted effective depolarization $[\Delta P] \approx 0.273 \cdot \Delta P \approx 3.5\%$

Adding the two contributions, we estimate almost 6.2% loss in effective polarisation from the collision.

Note that the depolarization for both processes mainly depends on N_y , which, for small Y , can be expanded as

$$N_y \approx \frac{5}{2} \frac{\alpha \sigma_z}{y \lambda_e} Y \left[\frac{1}{(1 + Y^{2/3})^{1/2}} \right] \approx 2 \frac{\alpha r_e N_b}{\sigma_x + \sigma_y} \quad (14)$$

Hence, it scales essentially with N_b/σ_x .

6. Polarization Measurement

In order to realize the advantage offered by polarization and since there is a significant depolarization in the collision, it appears important to measure the polarization before and after the collision. The usual polarimeter, pioneered at the SLC [33] and at several storage rings, utilizes laser-Compton back-scattering. The measured asymmetry is

$$A(E) = \frac{R(\rightarrow\rightarrow) - R(\rightarrow\leftarrow)}{R(\rightarrow\rightarrow) + R(\rightarrow\leftarrow)} = P_e P_y A_c(E) \quad (15)$$

where $A_c(E)$ denotes the known function of the Compton cross-section asymmetry and E the measured energy of the scattered electrons. The parameter P_y is the polarization of the laser, which can accurately be measured, and P_e the polarization of the electron (or positron) beam, which is to be determined. At the SLC, the systematic and statistical uncertainties in the polarization measurement were of the order of 1% or less. A precision of about 0.5% is foreseen for most future colliders, *e.g.*, in Ref. [34].

One potential problem for CLIC at 3 TeV is the large energy spread of the disrupted beam after the collision [35]. Care must be taken in the geometrical arrangement and location of the polarimeter, in order to avoid overlap of the low-energy electrons produced in the collision with those created by Compton scattering.

Figure 9 shows a schematic of the spent-beam line and post-IP polarimeter proposed for the NLC [9]. A similar layout may be adopted for CLIC. A chicane separates the disrupted particle beam from the beamstrahlung photons and oppositely charged pair particles, for diagnostics purposes. Here, is the natural location of the second polarimeter which measures the effective polarization of the disrupted e^\pm beam. To avoid background from the reaction $e^- \gamma \rightarrow e^- e^+$ the laser energy must be low, namely $E_\gamma < 522 \text{ eV}/E_e[\text{GeV}]$, where E_e is the initial electron energy. Hence, for CLIC at 3 TeV the photon energy should ideally be less or equal 0.3 eV.

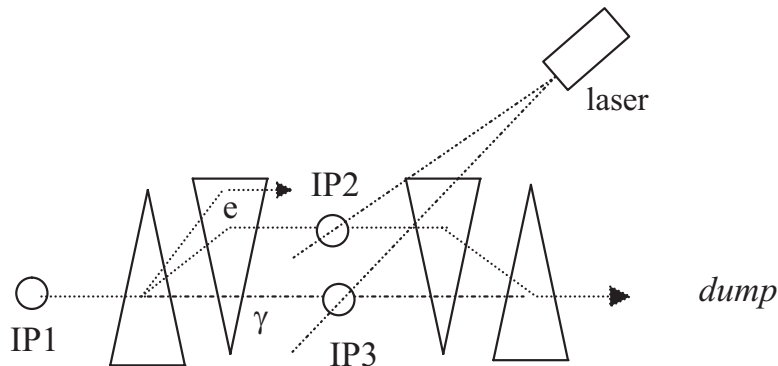


Figure 9: Schematic of NLC-type spent-beam diagnostics and post-IP laser polarimeter (J. Spencer, 1996).

7. Conclusions

A polarized photoinjector can provide an electron beam with a polarization of $P \approx 80\%$. The CLIC requirements on both charge and pulse current are relaxed compared with those proposed and thought feasible for NLC-II in 1996. Concerning the generation of a polarized positron beam we presently favor the Japanese scheme which is based on laser-Compton back scattering off an unpolarized electron beam. The basic parts of this concept are presently being tested experimentally at KEK. The scheme profits from the rapid developments in laser technology and promises to deliver a polarized positron beam with a polarization of $P \approx 60 - 80\%$. If the experimental tests of the Japanese scheme show unexpected problems, we can alternatively consider the helical undulator scheme that has been proposed for VLEPP and TESLA.

The spin transport for CLIC was estimated with analytical formulae and numerical spin tracking through the beam delivery system. It was found to be uncritical, with expected depolarization safely below 1%. However, for CLIC at 3 TeV, the depolarization during the collision will be noticeable. The total depolarization is about 25%, the effective luminosity-weighted loss is a more acceptable value of $[\Delta P] \approx 7\%$. Higher polarization may be attainable at the expense of reduced luminosity.

8. Acknowledgement

We thank M. Battaglia and A. De Roeck for suggesting this study, and G. Guignard, T. Kamitani, T. Omori, F. Ruggiero, D. Schulte, J. Urakawa, and I. Wilson for support and discussions.

References

- [1] P.L. Reinertsen, "Precise Measurement of the Weak Mixing Angle from Leptonic Polarization Asymmetries at the SLD Experiment," SLAC-PUB-8029 (1998).
- [2] R. Assmann, et al., "Spin Dynamics in LEP with 40-100 GeV Beams". Proc. Int. Spin Symposium SPIN2000. September 16- 20, 2000, Osaka, Japan.
- [3] H. Tang, et al., "The SLAC Polarized Electron Source," International Workshop on Polarized Beams and Polarized Gas Targets, Cologne, Germany, June 6-9, SLAC-PUB-6918 (1995).

- [4] S. Schreiber, "An RF Gun as Polarized Source for TESLA," TESLA 97-01 (1997).
- [5] G. Suberlucq, CLIC seminar, 5th October 2001.
- [6] T. Nakanishi, et al., "Highly Polarized Electron Source Development in Japan," APAC'98 Tsukuba (1998).
- [7] R. Alley et al., NIM A365, 1 (1995).
- [8] H. Tang et al., "Polarized Electron Sources for Future e^+ / e^- Linear Colliders," IEEE PAC 1997 Vancouver (1997).
- [9] "Zeroth Order Design Report for the Next Linear Collider," submitted to Snowmass 1996.
- [10] V.E. Balakin and A.A. Mikhailichenko, "VLEPP: The Conversion System for Obtaining Highly Polarized Electrons and Positrons," Preprint INP 79-85 (1979).
- [11] K. Floettmann, "Investigations Towards the Development of Polarized and Unpolarized High Intensity Positron Sources for Linear Colliders," DESY-93-161 (1993).
- [12] T. Kamitani, private communication (2000).
- [13] T. Omori, "A Polarized Positron Beam for Linear Colliders," 1st ACFA Workshop on Physics/Detector at the Linear Collider, KEK-Preprint 98-237 (1999).
- [14] T. Hirose, et al., "Polarized Positron Source for the Linear Collider, JLC," NIM A 455, p. 15 (2000).
- [15] T. Kotseroglou, et al., "Recent Developments in the Design of the NLC Positron Source," 1999 IEEE PAC, New York (1999).
- [16] A.P. Potylitsyn, "Laser Polarization of Positron Beam" (2001).
- [17] J. Clendenin, "Recent Advances in Electron and Positron Sources," 9th Workshop on Advanced Accelerator Concepts, SLAC-PUB-8465 (2000).
- [18] Ya.S. Derbenev, A.M. Kondratenko, E.L. Saldin, "Polarization of Electrons in Storage Rings by Circularly Polarized Electromagnetic Waves," NIM 165 pp. 201 (1979).
- [19] J. Urakawa, private communication (2001).
- [20] T. Omori, "A Concept of a Polarized Positron Source for a Linear Collider," International Conference on Lasers'99, Quebec, Canada, KEK Preprint 99-188 (2000).
- [21] H.A. Tolhoek, Rev. Mod. Phys. 28, pp. 277 (1956).
- [22] M. Minty, "Electron Beam Depolarization in a Damping Ring," PAC93 Washington D.C., SLAC-PUB-6114 (1993).
- [23] V. Bargmann, L. Michel, and V.L. Telegdi, "Precession of the Polarization of Particles Moving in a Homogeneous Electromagnetic Field". Phys. Rev. Lett. 2 (1959) 435.
- [24] F. Zimmermann, et al., "Final-Focus System for CLIC at 3 TeV," EPAC 2000, Vienna, CERN-SL-2000-057.
- [25] K. Oide, "Final Focus System with Odd Dispersion Scheme", HEACC'92, Hamburg, p. 2993 (1992).
- [26] P. Raimondi and A. Seryi, "A Novel Final Focus Design for High Energy Colliders", EPAC 2000, Vienna, p. 492.
- [27] F. Zimmermann, et al., "Final-Focus Schemes for CLIC at 3 TeV," HEACC01, Tsukuba, CERN-SL-2001-010 AP, and CLIC Note 476 (2001).
- [28] P. Tenenbaum, et al., "Studies of Beam Optics and Scattering in the Next Linear Collider Postlinac Collimation System," SLAC-PUB-8562 (2000).
- [29] H. Grote and C. Iselin, "The MAD Program (methodical accelerator design) version 8.4: User's reference manual," CERN-SL-90-13-AP-REV.2 (1990).
- [30] D. Schulte, private communication (1999).
- [31] K. Yokoya and P. Chen, "Beam-Beam Phenomena in Linear Colliders," Lecture at 1990 US-CERN School on Particle Accelerators, Hilton Head Island, South Carolina (1990).
- [32] K. Yokoya and P. Chen, "Depolarization due to Beam-Beam Interaction in Electron-Positron Linear Colliders," 8th International Symposium on High Energy Spin Physics, Minneapolis (1988).
- [33] M. Woods, "The Scanning Compton Polarimeter for the SLD Experiment," Workshop on High-Energy Electron Polarimeters, Amsterdam, September 1996, SLAC-PUB-7309 (1996).
- [34] V. Gharibyan et al., "The TESLA Compton Polarimeter," LC-DET-2001-047 (2001).
- [35] D. Schulte, "High-Energy Beam-Beam Effects in CLIC," IEEE PAC 1999, New York (1999).